Geophysical Research Letters

RESEARCH LETTER
10.1029/2023GL103548

Why Did the 2017 Kuroshio Large Meander Event Become the Longest in the Past 70 Years?

Bo Qiu[1], **Shuiming Chen**[1], **and Eitarou Oka**[2]

[1]Department of Oceanography, University of Hawaii at Manoa, Honolulu, HI, USA, [2]Atmosphere and Ocean Research Institute, The University of Tokyo, Kashiwa, Japan

Key Points:

- The Kuroshio south of Japan is known to vacillate between straight and large meander (LM) paths
- Started in August 2017, the on-going LM event has become the longest among the eight LM events detected since 1950
- This longevity is argued to be caused by highly stable dynamic state of the Kuroshio Extension after 2018 forced by the Pacific basin winds

Correspondence to:

B. Qiu,
bo@soest.hawaii.edu

Citation:

Qiu, B., Chen, S., & Oka, E. (2023). Why did the 2017 Kuroshio large meander event become the longest in the past 70 years? *Geophysical Research Letters*, *50*, e2023GL103548. https://doi.org/10.1029/2023GL103548

Received 3 MAR 2023
Accepted 8 MAY 2023

Author Contributions:

Conceptualization: Bo Qiu, Eitarou Oka
Data curation: Shuiming Chen
Formal analysis: Bo Qiu, Shuiming Chen
Funding acquisition: Bo Qiu, Eitarou Oka
Investigation: Bo Qiu, Shuiming Chen, Eitarou Oka
Methodology: Bo Qiu, Shuiming Chen, Eitarou Oka
Project Administration: Bo Qiu
Software: Shuiming Chen
Supervision: Bo Qiu
Visualization: Bo Qiu, Shuiming Chen
Writing – original draft: Bo Qiu
Writing – review & editing: Bo Qiu, Eitarou Oka

Abstract The Kuroshio south of Japan is known to vacillate between a straight and a large meander (LM) path. Since 1950, eight LM events have been observed with different durations. The most recent/on-going LM started in August 2017 and has become the longest event in record. By analyzing eddy-resolving sea surface height data and by adopting a wind-forced linear vorticity model, we demonstrate that the on-going LM is maintained by an exceptionally stable dynamic state of the Kuroshio Extension (KE) forced by wind stresses across the Pacific basin. The highly-stable KE system not only minimizes westward eddy perturbations from disrupting the upstream Kuroshio path, its strengthened southern recirculation gyre further helps to anchor the Kuroshio across the Izu Ridge. By contrasting the on-going event to the 2004–2005 event, we argue that the LM duration is more sensitive to the wind-forced KE dynamic state than the eastward Kuroshio transport south of Japan.

Plain Language Summary Occurrence of large meanders (LMs) by the Kuroshio south of Japan is a unique characteristic among the 5 western boundary currents in the wind-driven subtropical ocean gyres. The LM occurrence and durations have both been observed to be irregular and chaotic. While processes initiating a LM event have been widely examined, the factors controlling the LM duration remain less explored. Two LM events with drastically different durations took place after the global eddy-resolving sea surface height data from satellite altimeters became available. In contrast to the 2004–2005 LM event with a duration of 14 months, the on-going LM started in August 2017 and, by persisting for >67 months, has become the longest among the eight recorded events since 1950. This study investigated the processes responsible for the differing durations of these two LM events. It is found that the wind-forced stability of the Kuroshio Extension system east of the Izu Ridge plays a critical role in setting the LM's durations. This investigation is important because the Kuroshio LM impacts not only on fisheries south of Japan, but also synoptic weathers, such as typhoon paths, and climate in coastal areas facing the North Pacific Ocean.

1. Introduction

The Kuroshio is the western boundary current in the wind-driven North Pacific subtropical gyre (Imawaki et al., 2013; Kida et al., 2015; Qiu, 2019). While its upstream path is effectively constrained by coastal boundaries and the steep East China Sea continental slope, the Kuroshio path becomes less topographically restrained after it exits the Tokora Strait near 130°E (Figure 1a). In the deep Philippine Sea south of Japan, the Kuroshio path is known to exhibit bimodal fluctuations on interannual and longer timescales. During its "straight-path" years, as in 2010-14 shown in Figure 1b, the Kuroshio follows closely the southern coast of Japan and during the "large meander" (LM) years, as in 2018–2022 in Figure 1b, the Kuroshio takes an offshore detouring path with its southernmost latitude reaching 30°N. After crossing the meriodionally-aligned Izu Ridge along ∼140°E, the Kuroshio detaches from the coast and flows eastward as an inertial jet with prominent northern and southern recirculation gyres (Jayne et al., 2009; Nakano et al., 2008; Qiu et al., 2008). East of the Izu Ridge, the Kuroshio is renamed as the Kuroshio Extension (KE).

One proxy that captures faithfully the bimodal Kuroshio path changes south of Japan is the sea level difference measured at the Kushimoto (133.77°E, 33.48°N) and Uragami (135.90°E, 35.56°N) tide gauge stations (Kawabe, 1980, 1995; see Figure 1b for their locations). When the Kuroshio is in a straight-path (LM) state, its in-shore (off-shore) path causes the Kushimoto-Uragami sea level difference to increase (drop). Other observed quantities, such as the mean Kuroshio distance from the coast, have also been used in the past to quantify the Kuroshio path changes (for an updated review, readers are referred to Qiu & Chen, 2021). Since 1950, eight

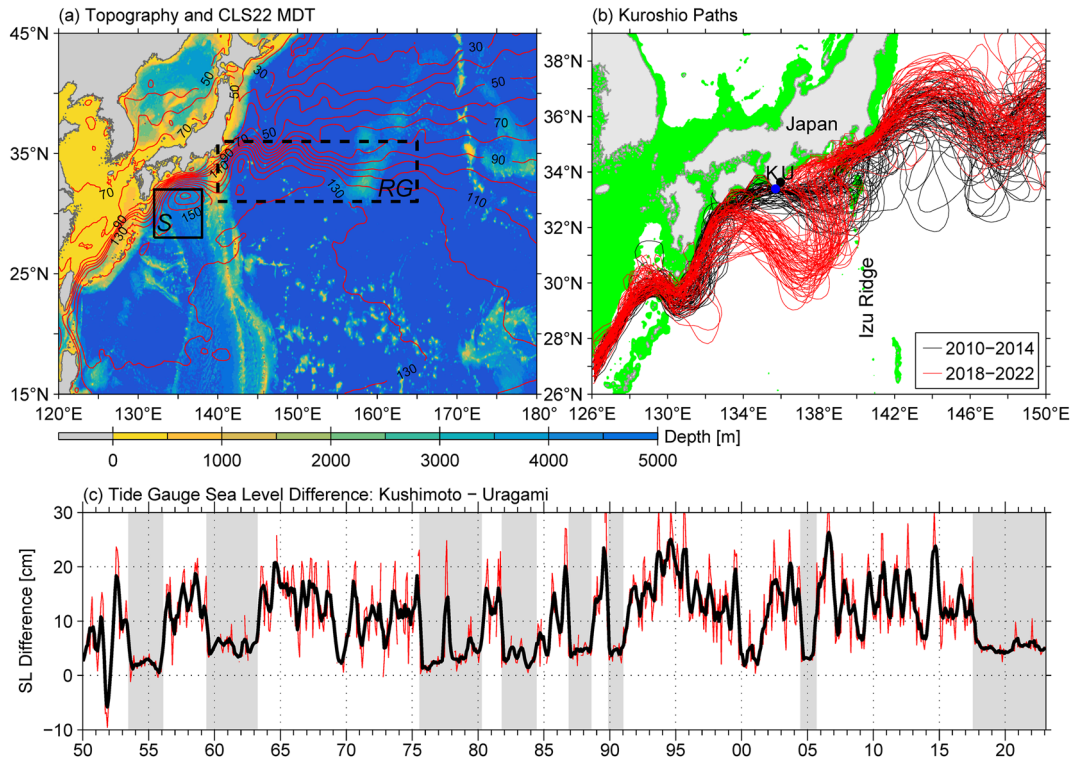

Figure 1. (a) Mean sea surface height distribution (cm) in the western North Pacific by Jousset et al. (2022). Colors show the bathymetry from Smith and Sandwell (1994). *S* box denotes the area where Sverdrup transport is evaluated and dashed RG box indicates the KE recirculation gyre region. (b) Monthly Kuroshio/KE paths during the straight-path years (2010–2014, black lines) versus large-meander years (2018–2022, red lines). Green shade denotes areas shallower than 500 m. K and U denote tide gauge station Kushimoto and Uragami, respectively. (c) Time series of sea level difference of Kushimoto-Uragami. Black line denotes the time series after 5-month running mean. Shaded windows denote the Kuroshio large meander periods.

Kuroshio LM events have occurred with both of their occurrence and durations appearing random and irregular (Figure 1c). The bimodal Kuroshio path variability exerts a significant impact not only on regional physical oceanic processes (Nishikawa et al., 2023; Oka et al., 2021; Qiu et al., 2020; Sugimoto et al., 2020), but also on fisheries, typhoon paths and coastal climate (Chang et al., 2019; Lizarbe Barreto et al., 2021; Nakamura et al., 2012; Sugimoto et al., 2021).

Research on dynamics underlying the bimodal Kuroshio path variability has a long history. Comprehensive reviews on the past theoretical, modeling and data analysis studies can be found in Tsujino et al. (2013), Usui (2019), and Qiu and Chen (2021). Two aspects of the chaotic Kuroshio path variability are of particular interest: one is the LM initiations and the other, its durations. With regard to the LM initiations, many existing studies have found that high mesoscale eddy activity along the Subtropical Countercurrent (STCC) band of 18°–28°N in the western North Pacific Ocean plays critical and inducive roles. Specifically, increased mesoscale eddy variability favors the generation of cyclonic-anticyclonic eddy pairs: the cyclonic eddy often triggers small-amplitude cyclonic meander of the Kuroshio path southeast of Kyushu and the succeeding anticyclonic eddy facilitates the stalling/growth of cyclonic-eddy triggered meandering path. For seven out of the eight LM events identified in Figure 1c, it is found that they were preceded by heightened mesoscale eddy activity due to interannually increased Ekman flux convergence along the STCC band (Qiu & Chen, 2021).

Compared to the initiation of a LM event, our understanding about the processes dictating the *duration* of a LM event remains less well established. Several past studies have argued that the magnitude of the eastward Kuroshio transport south of Japan acts as an important factor. Based on sensitivity experiments using a data-assimilated model, Usui et al. (2013) found that a reduced Kuroshio transport can result in a longer LM duration due to stationary Rossby lee waves with a shorter zonal wavelength being more easily maintained south of Japan. With the accumulation of high-precision satellite altimeter measurements of the past three decades and our overall

better understanding about the low-frequency Kuroshio/KE variability, we are now in a favorable position to re-examine the issue relating to the LM duration changes. Fortuitously, two LM events with drastically different durations occurred in the satellite altimetry era. The 2004/05 LM event, as seen in Figure 1c, lasted for only 14 months from July 2004 to August 2005. In contrast, the most recent/on-going LM started in August 2017 and, by persisting for >67 months, has become the longest event in observational record since 1950.

By analyzing the eddy-resolving altimetry data and by adopting the wind-forced linear vorticity model, we explore in this study processes that contribute to the contrasting durations of the 2004–2005 versus 2017-present LM events. Due to the planetary β effect, mesoscale oceanic perturbations propagate westward (Chelton et al., 2011). With the Kuroshio south of Japan located to the west of the KE, our particular attention is paid to how the wind-forced KE dynamic state changes can affect the LM duration through the planetary β effect and interaction with the Izu Ridge. In addition to the KE impact from east of the Izu Ridge, relevance of changes in eastward Kuroshio transport west of the Izu Ridge on the LM duration will also be discussed.

2. Observational Data Sets

To examine the Kuroshio/KE variability in connection to the LM events, we use the global sea surface height (SSH) data set processed by Ssalto/Duacs and distributed by the Copernicus Marine and Environment Monitoring Service. This data set merges along-track SSH measurements from all satellite altimeter missions and has a 1-day temporal and a 1/4° spatial resolution. The data period analyzed in this study extends from January 1993 to December 2022.

To relate the oceanic SSH and Sverdrup transport variability to that of the atmospheric forcing, we utilize the monthly surface wind stress data from the European Centre for Medium–Range Weather Forecasts (ECMWF) ERA-5 reanalysis product. The ECMWF ERA-5 data have the same spatial resolution of 0.25° as the altimeter-derived SSH data and are available from January 1950 to September 2022.

3. Results

3.1. Kuroshio Extension Variability

Following our previous study (Qiu & Chen, 2005), we adopt four dynamic quantities to quantify the low-frequency variability of the KE system east of the Izu Ridge. Figure 2a shows the KE pathlength integrated from 141°E to 153°E based on the SSH data from 1993 to 2022 (see Figure 1b for representative paths). A short (long) pathlength indicates a stable (unstable) KE dynamic state. Figures 2b and 2c show the surface eastward transport and latitudinal position of the KE averaged from 141°E to 165°E, respectively, and Figure 2d shows the intensity of KE's southern recirculation gyre inferred from the area where absolute SSH value exceeds 2.0 m (see Qiu & Chen, 2005 for details). In its unstable state as denoted by black bars in Figures 2a–2d, the KE jet tends to have a reduced eastward transport, a southerly latitudinal position, and a weakened southern recirculation gyre. The reverse is true when the KE switches to a stable state. Because these quantities are temporally correlated, they can be combined (by reversing the sign of pathlength and averaging the four time series normalized by their respective standard deviations) to form a *KE index* to succinctly represent the dynamic state of the observed KE system (Figure 2e). Thus formulated, a positive KE index signifies a stable dynamic state and a negative index, an unstable dynamic state. Consistent with the findings in Qiu et al. (2014), this KE index is correlated favorably with the anomalous SSH signals in the KE southern recirculation gyre box of 31°–36°N, 140°-165°E (compare Figure 2e with Figure 2f; the two time series have a linear correlation coefficient $r = 0.91$). In other words, exploring the low-frequency KE variability becomes equivalent to quantifying the SSH changes in the *RG* box shown in Figure 1a.

As noted by many previous studies, the KE system in the past four decades have fluctuated between a stable and an unstable dynamic state on the quasi-decadal timescales (Joh & Di Lorenzo, 2019; Qiu & Chen, 2005; Sasaki et al., 2013; Taguchi et al., 2007). The transition between the two dynamic states has been shown to be induced by arrivals of SSH anomalies in the KE recirculation gyre that have been generated in the eastern Pacific (170°W-140°W) due to Pacific decadal oscillation (PDO)-related wind forcing. For example, with a delay of ∼3 years, the KE system in late 2016 and early 2017 transitioned to an unstable state (Figure 3a) due to the incoming *negative* SSH anomalies from the eastern North Pacific caused by the positive PDO wind forcing after

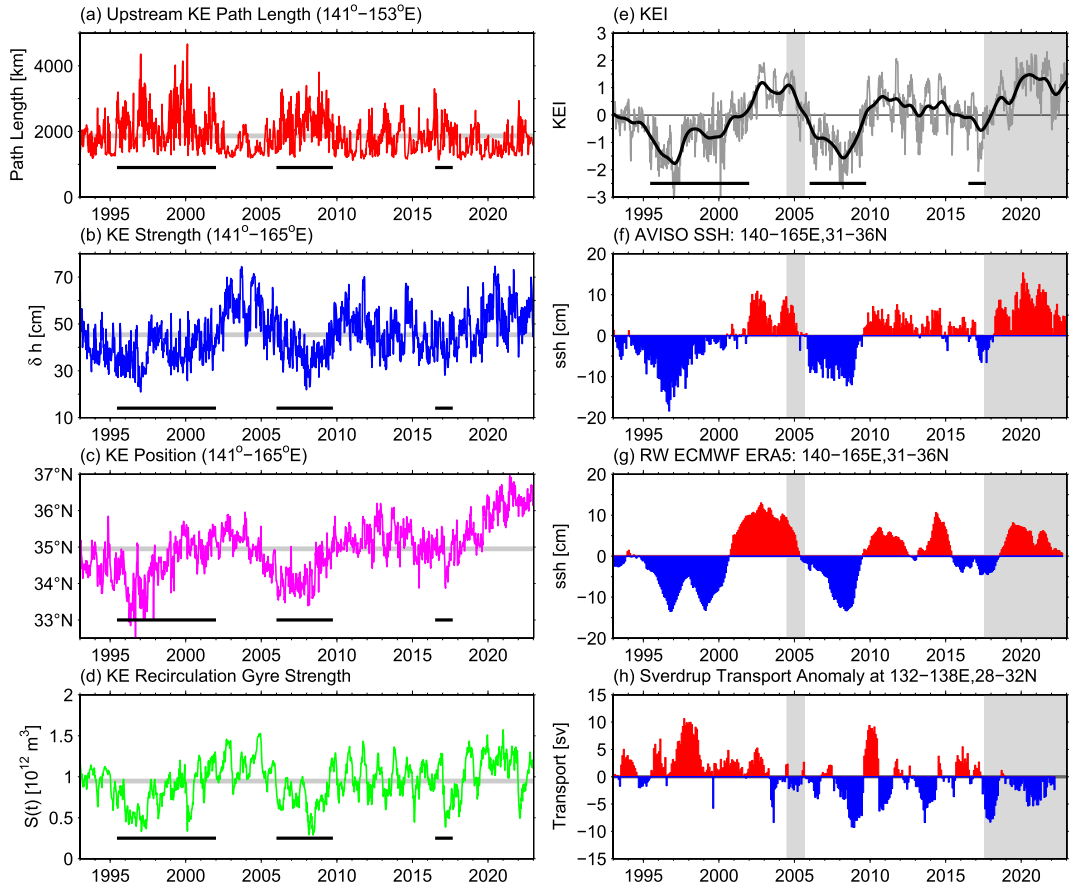

Figure 2. Time series of (a) KE pathlength integrated from 141° to 153°E, (b) sea surface height (SSH) difference across the KE jet from 141° to 165°E, (c) latitudinal KE position from 141° to 165°E, (d) intensity of the KE recirculation gyre, and (e) synthesized KE index. Black bars denote the periods when the KE is in unstable state. Thick black line in (e) shows the low-passed KE index by a Gaussian filter with a 4-month decay scale. Time series of (f) SSH anomalies in the *RG* box, (g) SSH anomalies in the *RG* box hindcasted by the linear vorticity model, and (h) Sverdrup transport anomalies in the *S* box south of Japan.

2014 (Figures 3b and 3c). This unstable state, however, is disrupted due to the LM occurrence in August 2017 that has forced the KE path to shift poleward instead of equatorward (see Figure 2c after 2017; Qiu et al., 2020). Following this reversal from an unstable to a stable state of the KE system, the SSH anomalies in the *RG* box continue to rise, reaching a positive value that exceeds the two preceding stable periods of the KE in 2001–2005 and 2010–2015.

It is important to emphasize that this unprecedented stabilization of the KE system after 2018 are *not* solely an outcome of the on-going Kuroshio LM event. As shown in Figure 3b, a significant portion of the observed positive SSH anomalies in the western *RG* segment that contributed to the stabilized KE dynamic state after 2018 are observed to have originated in the eastern North Pacific. To quantify this contribution, we evaluate the SSH changes in the KE recirculation gyre box using the ERA5 wind stress data based on the wind-forced linear vorticity model (Qiu et al., 2014):

$$\frac{\partial \eta}{\partial t} - C_R \frac{\partial \eta}{\partial x} = -\frac{g'}{g} \nabla \times \left(\frac{\boldsymbol{\tau}}{\rho_0 f} \right) \tag{1}$$

where η is the wind-induced SSH anomaly, C_R the long baroclinic Rossby wave speed (Chelton et al., 2008), g the gravity constant, g' (=0.04 m/s^2) the reduced gravity, f the Coriolis parameter, ρ_0 (=1,023 kg/m^3) the reference density, and $\boldsymbol{\tau}$ the monthly wind stress vector. Compared to the observed ~10 cm SSH anomalies in 2018-22 shown in Figures 2f and 2g reveals that nearly half (~5 cm) of these positive SSH anomalies are produced by the

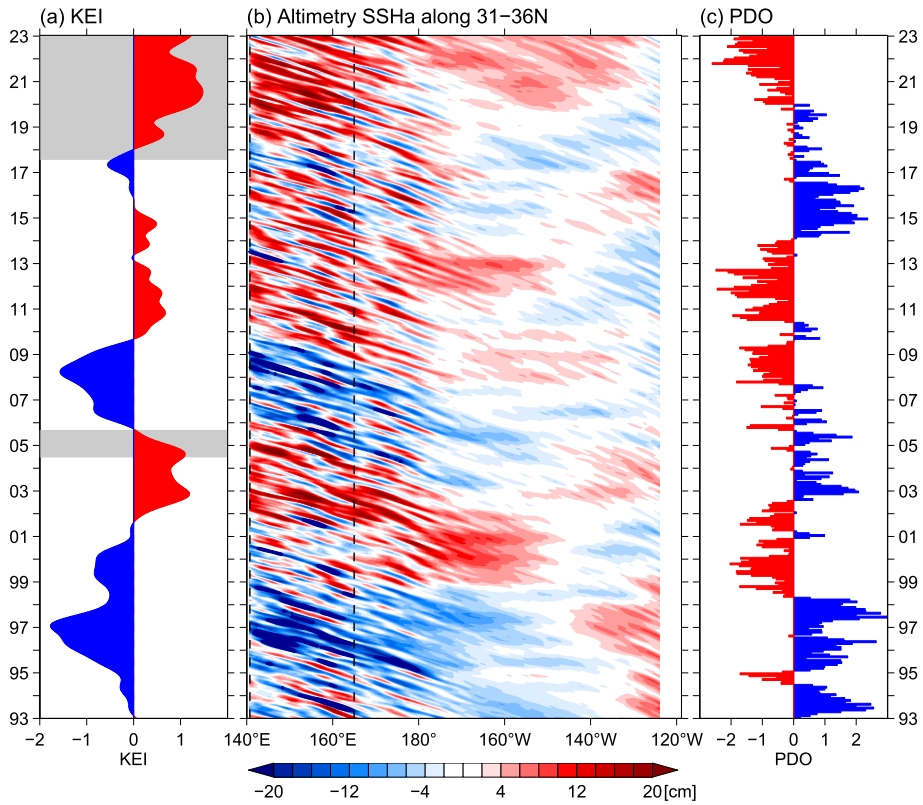

Figure 3. (a) KE index time series (same as Figure 2e). (b) Time-longitude plot of sea surface height anomalies along the 31°–36°N band. Dashed lines denote the *RG*-box segment. To focus on the regional variability, the 3.3 mm/year global-mean sea level rise trend is removed. (c) PDO index.

surface wind stress forcing across the North Pacific basin and are *independent* of the Kuroshio LM event south of Japan. In other words, the highly-stable KE state observed in the past 5 years is a combined response to the occurrence of the Kuroshio LM west of the Izu Ridge and the forcing by the interior wind stresses across the eastern North Pacific.

In contrast to the latest LM event, the short-lived 2004–2005 LM started when the KE system was in a stable dynamic state. As indicated in Figure 2e, the LM disappeared in mid 2005 after the KE index switched from positive to negative. Similar to the 2017-present LM event, Figures 2g, 3b, and 3c reveal that the KE dynamic state and its transition are largely controlled by the westward-propagating SSH anomalies generated by the PDO-related surface wind forcing in the eastern North Pacific.

3.2. Impacts on LM Duration

What are the impacts of the differing KE dynamic states on the LM duration? To address this question, we plot in Figure 4 the yearly eddy kinetic energy anomaly distributions in the Kuroshio/KE regions. Here, eddy kinetic energy is calculated geostrophically from the SSH data and its anomaly is defined relative to the mean eddy kinetic energy level of 1993–2022. For the 2004-05 LM event, it can be seen that the eddy kinetic energy level is anomalously high in 2005 and onward in the KE region south of ~35°N. In contrast, the eddy kinetic energy level is anomalously low in the southern KE region in 2018–2222 following the LM occurrence in 2017. Dynamically, these changes in the eddy kinetic energy field are not surprising as they are another manifestation (in addition to those shown in Figures 2a–2d) between the stable versus unstable state of the KE system.

Figure 5a shows that a deep channel with depths >1,500 m exists near 34°N across the Izu Ridge. When it assumes a LM path, the Kuroshio tends to exit through this deep channel to the open Pacific Ocean (see, e.g., top panel in Figure 5b). South of 34°N, the Izu Ridge shoals between 32.5° and 34°N and when the Kuroshio overrides this shallower ridge segment, its path west of the Izu Ridge is often perturbed due to the planetary β

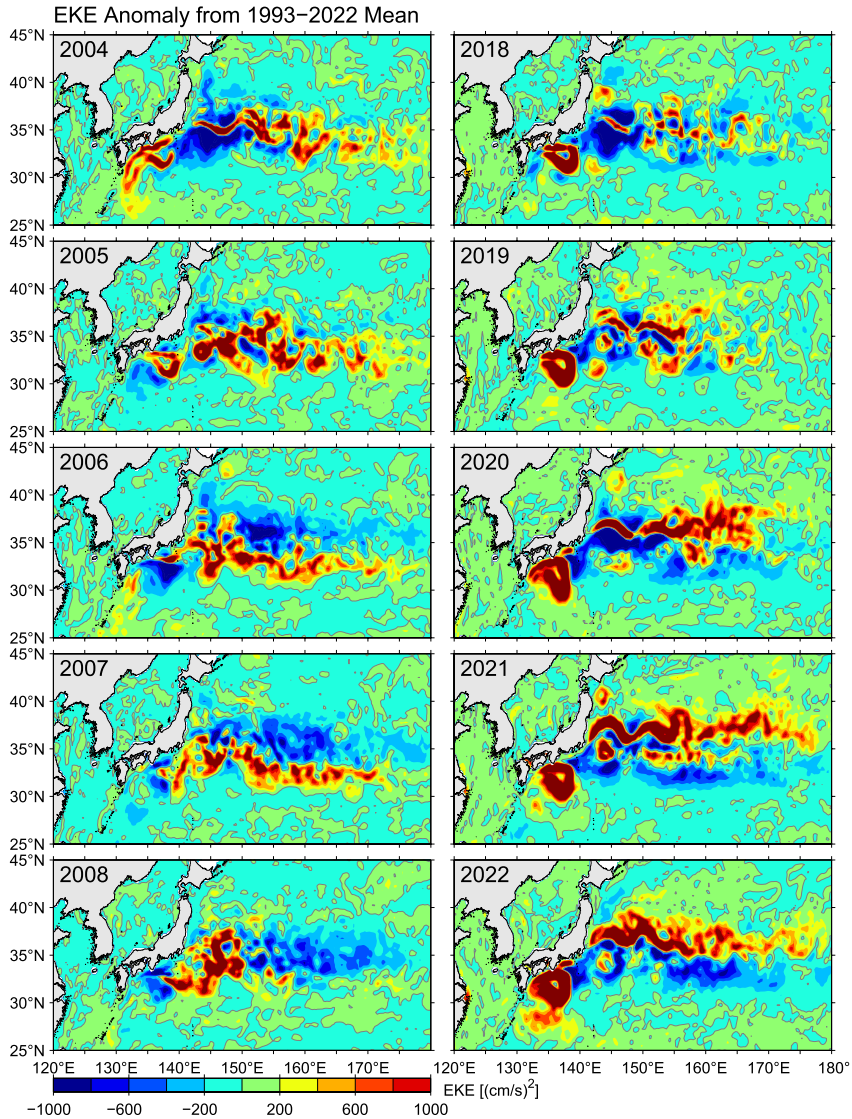

Figure 4. Yearly eddy kinetic energy anomaly distributions in the Kuroshio/KE region. Here, anomalies are defined as deviations from the 1993–2022 mean eddy kinetic energy value.

effect. When the eddy kinetic energy level increased in the KE region south of 35°N after 2005 (Figure 4, left column), westward-propagating mesoscale perturbations originated in the downstream KE region were able to force the Kuroshio path laterally onto the shallower segment of the Izu Ridge (to be detailed in next section). This destabilizes the meandering path of the Kuroshio south of Japan, making the 2004–2005 LM a short-live event. Following the LM initiation in August 2017, on the other hand, the eddy kinetic energy level in the KE region south of 35°N is subdued (Figure 4, right column) and this reduces disturbances to the Kuroshio path over the Izu Ridge (recall red pathlines in Figure 1b). It is this difference in the wind-forced dynamic state of the KE that, we believe, contributed to the starkly different durations between the Kuroshio LM events in 2004–2005 versus 2017-present.

4. Discussion and Summary

Persistence of a LM event requires the Kuroshio over the Izu Ridge to pass through the deep channel near 34°N (Figure 1b). By analyzing the eddy-resolving SSH data and by adopting the wind-forced linear vorticity model, we have identified the KE dynamic state forced by wind stresses across the Pacific basin to be a determinant factor. By strengthening the southern recirculation gyre and by shifting its axis northward, a stable KE dynamic

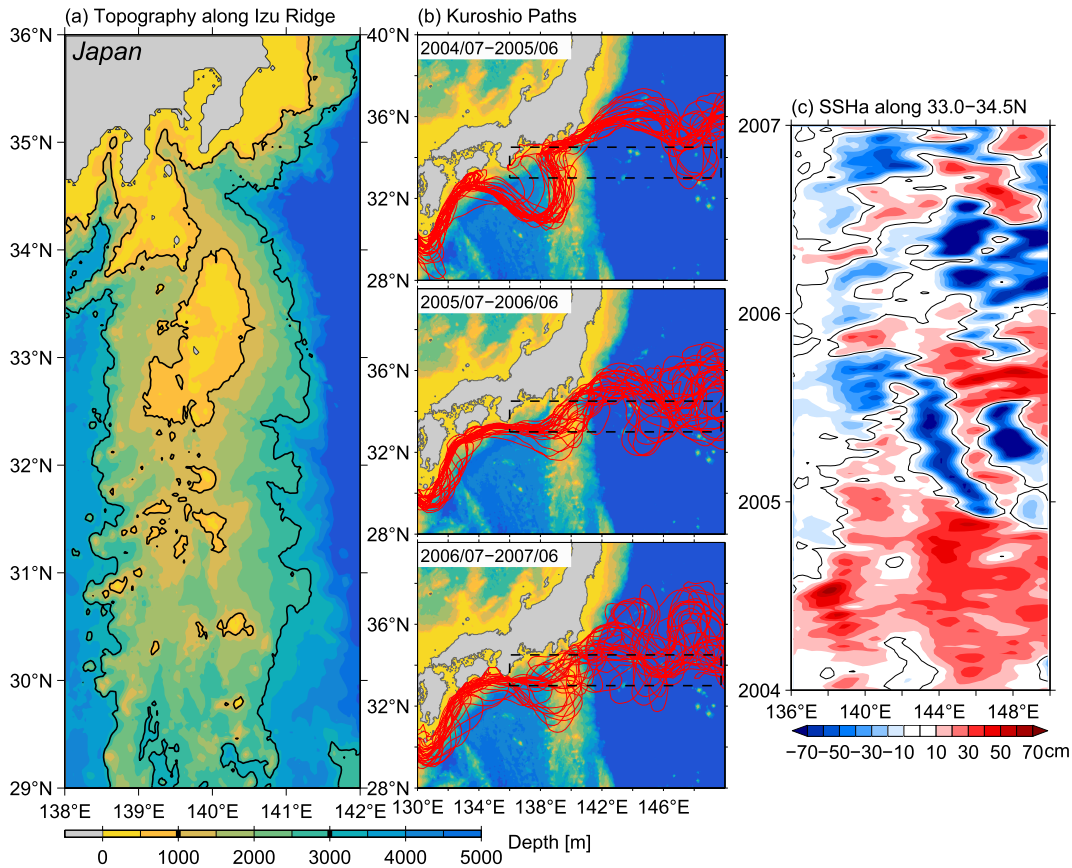

Figure 5. (a) Detailed bathymetry around the Izu Ridge. Thick contours denote 1,000 m & 3,000 m isobaths. (b) Biweekly Kuroshio/KE paths during 2004/07–2005/06 (top), 2005/07–2006/06 (mid), and 2006/07–2007/06 (bottom). (c) Time-longitude plot of sea surface height anomalies along 33.0°–34.5°N across the Izu Ridge. The analyzed area is indicated by dashed boxes in (b).

state, for example, corresponds to anomalously low eddy kinetic energy level and favors to anchor the Kuroshio to pass through the deep channel over the Izu Ridge.

As noted in the Introduction, the magnitude of the eastward Kuroshio transport has been argued by past studies based on stationary Rossby lee waves to be an important contributor to the length of a LM event. To examine the relationship between the eastward Kuroshio transport variations and the duration of the recent two LM events, we follow Usui et al. (2013) and calculate the Sverdrup transport anomaly time series based on the ERA5 wind stress data averaged in 132°–138°E, 28°–32°N (the *S* box in Figure 1a). By regarding the Kuroshio to be a compensating flow to the wind-driven interior circulation, this Sverdrup transport value serves as a proxy for the eastward Kuroshio transport south of Japan. As shown in Figure 2h, while the Sverdrup transport was close to its time-mean value (44.5 Sv) during the 2004–2005 LM period, it is reduced by 4 ~ 5 Sv, or about 10% of the time-mean value, after the 2017 LM occurrence. This transport difference is consistent with the Usui et al.'s (2013) findings that the LM duration tends to lengthen when the eastward Kuroshio transport south of Japan is reduced.

It is worth emphasizing that the reduced Sverdrup transport shown in Figure 2h and the wind-forced stable state of the KE shown in Figure 2g after 2018 are *not* a coincident. The dominant surface wind stress forcing and the Sverdrup transport in the midlatitude North Pacific basin are related to the PDO phases. During the negative PDO phase, for example, negative and positive wind stress curl anomalies tend to appear north and south of ~32°N in the central-eastern North Pacific basin (see Figure 2 in Qiu, 2003). Such a meridionally-dipolar wind stress curl forcing would lead to a stable dynamic state of the KE system to the north of 32°N and, at the same time, reduce the Sverdrup transport in the 28°–32°N band south of Japan. With the PDO phase switching from positive to negative in recent years after 2018 (Figure 3c), this is indeed what happened.

Given that the Sverdrup transport in the upstream Kuroshio south of Japan and the wind-forced KE dynamic state can both affect the duration for a LM event, a question arising naturally is which of these two processes play a more important role. Some hints to the answer of this question can be gained by taking a close look at the decaying process of the 2004–2005 LM event over the Izu Ridge. Note that if the LM duration is controlled by the upstream Kuroshio transport changes, we can expect the Kuroshio path variability to start south of Japan and be advected *eastward* to over the Izu Ridge. On the other hand, if the LM duration is dictated by the KE dynamic state changes, the Kuroshio path variability should first emerge in the downstream KE region and then propagate *westward* via the planetary β effect. Examination of the SSH anomaly signals along the 33.0°–34.5°N band (Figure 5c) reveals that the LM demise in August 2005 corresponds to the appearance of negative SSH anomalies, or a southward migration by the Kuroshio path, over the Izu Ridge. These negative SSH anomalies emerged *first* in the 144°–148°E segment in early 2005 as a result of the positive-phased PDO wind forcing that brought in the wind-forced negative SSH anomalies into the KE region (Figures 3b and 3c). After propagating westward, these anomalies perturbed the Kuroshio path southward over the Izu Ridge and destabilized the meandering Kuroshio path south of Japan (see mid & lower panels in Figure 5b). Notice that throughout 2005, no SSH anomalies over the Izu Ridge could be seen to have initiated from the upstream Kuroshio region *west* of 140°E in Figure 5c.

Due to the limitation of the available eddy-resolving SSH data, we have in this study focused on the roles played by the KE dynamic state and mesoscale eddies upon the durations of the recent two LM events. It will be of interest for future studies to quantify the contributions to the durations of other LM events from changes in the upstream Kuroshio transport versus the KE dynamic state based on eddy-resolving OGCM simulations and/or data-assimilated products. In light of the decay processes of the 2004–2005 LM presented in Figure 5, it will also be of interest to see if the on-going LM event would demise similarly when the wind-forced KE dynamic state switches from the current stable state to a future unstable state.

Data Availability Statement

All data used in this study are publicly accessible. The PDO time series is available at https://www.ncei.noaa.gov/access/monitoring/pdo/, the merged satellite altimeter data are available at https://doi.org/10.48670/moi-00148, and the ECMWF ERA-5 reanalysis data are accessible from https://doi.org/10.24381/cds.f17050d7.

Acknowledgments
We are grateful to the two anonymous reviewers for their constructive comments. B.Q. and S.C. acknowledge support from NSF Grant 2019312 and NASA OSTST Grant 80NSSC21K1186. E.O. acknowledges support from MEXT Grant JP19H05700.

References

Chang, Y.-L., Miyazawa, Y., Miller, M. L., & Tsukamoto, K. (2019). Influence of ocean circulation and the Kuroshio large meander on the 2018 Japanese eel recruitment season. *PLoS One*, *14*(9), e0223262. https://doi.org/10.1371/journal.pone.0223262

Chelton, D. B., de Szoeke, R. A., Schlax, M. G., Naggar, K. E., & Siwertz, N. (2008). Geographical variability of the first baroclinic Rossby radius of deformation. *Journal of Physical Oceanography*, *28*(3), 433–460. https://doi.org/10.1175/1520-0485(1998)028<0433:gvotfb>2.0.co;2

Chelton, D. B., Schlax, M. G., & Samelson, R. M. (2011). Global observations of nonlinear mesoscale eddies. *Progress in Oceanography*, *91*(2), 167–216. https://doi.org/10.1016/j.pocean.2011.01.002

Imawaki, S., Bower, A. S., Beal, L., & Qiu, B. (2013). Western boundary currents. In G. Siedler, S. M. Griffies, W. J. Gould, & J. Church (Eds.), *Ocean circulation and climate—A 21st century perspective* (2nd ed., pp. 305–338). Academic Press.

Jayne, S., Hogg, N., Waterman, S., Rainville, L., Donahue, K., Watts, D., et al. (2009). The Kuroshio Extension and its recirculation gyres. *Deep-Sea Research*, *56*(12), 2088–2099. https://doi.org/10.1016/j.dsr.2009.08.006

Joh, Y., & Di Lorenzo, E. (2019). Interactions between Kuroshio Extension and Central Tropical Pacific lead to preferred decadal timescale oscillations in Pacific climate. *Scientific Reports*, *9*(1), 13558. https://doi.org/10.1038/s41598-019-49927-y

Jousset, S., Mulet, S., Wilkin, J., Greiner, E., Dibarboure, G., & Picot, N. (2022). *New global mean dynamic topography CNES-CLS-22 combining drifters, hydrological profiles and high frequency radar data*. Ocean Surface Topography Science Team. https://doi.org/10.24400/527896/a03-2022.3292

Kawabe, M. (1980). Sea level variations around the Nansei Islands and the large meander in the Kuroshio south of central Japan. *Journal of the Oceanographical Society of Japan*, *36*(4), 227–235. https://doi.org/10.1007/bf02070336

Kawabe, M. (1995). Variations of current path, velocity, and volume transport of the Kuroshio in relation with the large meander. *Journal of Physical Oceanography*, *25*(12), 3103–3117. https://doi.org/10.1175/1520-0485(1995)025<3103:vocpva>2.0.co;2

Kida, S., Mitsudera, H., Aoki, S., Guo, X., Ito, S. i., Kobashi, F., et al. (2015). Oceanic fronts and jets around Japan: A review. *Journal of Oceanography*, *61*(5), 469–497. https://doi.org/10.1007/s10872-015-0283-7

Lizarbe Barreto, D. A., Chevarria Saravia, R., Nagai, T., & Hirata, T. (2021). Phytoplankton increase along the Kuroshio due to the large meander. *Frontiers in Marine Science*, *8*. https://doi.org/10.3389/fmars.2021.677632

Nakamura, H., Nishina, A., & Minobe, S. (2012). Response of storm tracks to bimodal Kuroshio path states south of Japan. *Journal of Climate*, *25*(21), 7772–7779. https://doi.org/10.1175/jcli-d-12-00326.1

Nakano, H., Tsujino, H., & Furue, R. (2008). The Kuroshio Current system as a jet and twin "relative" recirculation gyres embedded in the Sverdrup circulation. *Dynamics of Atmospheres and Oceans*, *45*(3–4), 135–164. https://doi.org/10.1016/j.dynatmoce.2007.09.002

Nishikawa, H., Oka, E., & Sugimoto, S. (2023). Subtropical Mode Water in a recent persisting Kuroshio large-meander period: Part II—formation and temporal evolution in the Kuroshio recirculation gyre off Shikoku. *Journal of Oceanography*. https://doi.org/10.1007/s10872-023-00689-2

Oka, E., Nishikawa, H., Sugimoto, S., Qiu, B., & Schdeider, N. (2021). Subtropical mode water in a recent persisting Kuroshio large-meander period: Part I -- formation and advection over the entire distribution. *Journal of Oceanography*, *77*(5), 781–795. https://doi.org/10.1007/s10872-021-00608-3

Qiu, B. (2003). Kuroshio Extension variability and forcing of the Pacific decadal oscillations: Responses and potential feedback. *Journal of Physical Oceanography*, *33*(12), 2465–2482. https://doi.org/10.1175/2459.1

Qiu, B. (2019). In J. K. Cochran, H. Bokuniewicz, & P. Yager (Eds.), *Kuroshio and Oyashio currents. Encyclopedia of Ocean Sciences* (3rd ed., pp. 384–394). Academic Press.

Qiu, B., & Chen, S. (2005). Variability of the Kuroshio Extension jet, recirculation gyre, and mesoscale eddies on decadal time series. *Journal of Physical Oceanography*, *35*(11), 2090–2103. https://doi.org/10.1175/jpo2807.1

Qiu, B., & Chen, S. (2021). Revisit of the occurrence of the Kuroshio large meander south of Japan. *Journal of Physical Oceanography*, *51*, 3679–3694.

Qiu, B., Chen, S., Hacker, S. P., Hogg, N., Jayne, S., & Sasaki, H. (2008). The Kuroshio Extension northern recirculation gyre: Profiling float measurements and forcing mechanism. *Journal of Physical Oceanography*, *38*(8), 1764–1779. https://doi.org/10.1175/2008jpo3921.1

Qiu, B., Chen, S., Schneider, N., Oka, E., & Sugimoto, S. (2020). On reset of the wind-forced decadal Kuroshio Extension variability in late 2017. *Journal of Climate*, *33*(24), 10813–10828. https://doi.org/10.1175/jcli-d-20-0237.1

Qiu, B., Chen, S., Schneider, N., & Taguchi, B. (2014). A coupled decadal prediction of the dynamic state of the Kuroshio Extension system. *Journal of Climate*, *27*(4), 1751–1764. https://doi.org/10.1175/jcli-d-13-00318.1

Sasaki, Y. N., Minobe, S., & Schneider, N. (2013). Decadal response of the Kuroshio Extension jet to Rossby waves: Observation and thin-jet theory. *Journal of Physical Oceanography*, *43*(2), 442–456. https://doi.org/10.1175/jpo-d-12-096.1

Smith, W. H. F., & Sandwell, D. T. (1994). Bathymetric prediction from dense altimetry and sparse shipboard bathymetry. *Journal of Geophysical Research*, *99*, 2180–21824.

Sugimoto, S., Qiu, B., & Kojima, A. (2020). Marked coastal warming off Tokai attributable to Kuroshio large meander. *Journal of Oceanography*, *76*(2), 141–154. https://doi.org/10.1007/s10872-019-00531-8

Sugimoto, S., Qiu, B., & Schneider, N. (2021). Local atmospheric response to the Kuroshio Large Meander path in summer and its remote influence on the climate of Japan. *Journal of Climate*, *34*(9), 3571–3589. https://doi.org/10.1175/jcli-d-20-0387.1

Taguchi, B., Xie, S. P., Schneider, N., Nonaka, M., Sasaki, H., & Sasai, Y. (2007). Decadal variability of the Kuroshio extension: Observations and an eddy-resolving model hindcast. *Journal of Climate*, *20*(11), 2357–2377. https://doi.org/10.1175/jcli4142.1

Tsujino, H., Nishikawa, S., Sakamoto, K., Usui, N., Nakano, H., & Yamanaka, G. (2013). Effects of large-scale wind on the Kuroshio path south of Japan in a 60-year historical OGCM simulation. *Climate Dynamics*, *41*(9–10), 2287–2318. https://doi.org/10.1007/s00382-012-1641-4

Usui, N. (2019). Progress of studies on Kuroshio path variations south of Japan in the past decade. In T. Nagai, H. Saito, K. Suzuku, & M. Takahashi (Eds.), *Kuroshio current: Physical, biological and ecosystem dynamics*. *Geophysical Monograph 243*.

Usui, N., Tsujino, H., Nakano, H., & Matsumoto, S. (2013). Long-term variability of the Kuroshio path south of Japan. *Journal of Oceanography*, *69*(6), 647–670. https://doi.org/10.1007/s10872-013-0197-1